# Centers of Approximate Spherical Symmetry and Radial Symmetry Graphs

A.Giachetti[1] and C.Lovato[2]

[1]Department of Computer Science, University of Verona, Italy
[2]Department of Neurological, Neuropsychological, Morphological and Movement Sciences, University of Verona, Italy

**Abstract**
*In this paper we propose the possible use of a new type of salient points we call CASS (Centers of Approximate Spherical Symmetry) that are extracted from the Multiscale Area Projection transform described in [GL12]. In particular, we show that it is possible to build graphs joining these points following maximal values of the MAPT (Radial Symmetry Graphs) and that these graphs can be used to extract relevant shape properties (e.g. intrinsic symmetries) or to establish point correspondences on models robustly against holes, topological noise and articulated deformations.*

Categories and Subject Descriptors (according to ACM CCS): I.2.10 [Computer Graphics]: Vision and Scene Understanding—Shape

## 1. Introduction

Recent advances in 3D capture technologies boosted research on geometry processing algorithms able to capture local and global properties and that can be useful to analyze, measure, compare and recover acquired shapes.

Shapes are often characterized locally and globally by using salient points on surfaces, and trying to characterize their distribution [SF06], or by computing curve skeletons [CSM07] or medial axis transforms [MGP10], that are, however, difficult to handle in case of noise, holes and topological changes. In this paper we propose a new characterization based on volumetric salient points related to spherical symmetry, that can be captured by the Multiscale Area Projection Transform [GL12] that can be connected by paths following maximal radial symmetry defining a new structure we call "Radial Symmetry Graph". We believe that this representation could be extremely useful to perform tasks like shape retrieval, robust correspondence on shapes and intrinsic symmetry detection and we give some ideas on how we plan to apply it to demonstrate it experimentally.

## 2. Multiscale Area Projection Transform

The MAPT [GL12] is a function measuring an approximate degree of radial (actually spherical) symmetry of a 3D shape at different scales. Its definition is simple: given a radius $R$, the parallel surfaces of the input model at distance $R$ are computed and the Area Projection transform $APT(x,\sigma)$ in a point $\vec{x}$ is estimated as the area of the part of the original surface creating parallel surfaces that fall inside a sphere of radius $\sigma$ (see Fig.1):

$$APT(\vec{x},S,R,\sigma) = Area(T_R^{-1}(k_\sigma(\vec{x}) \subset T_R(S,\vec{n}))) \quad (1)$$

where $T_R(S,\vec{n})$ is the transform creating the parallel surface at distance $R$. If the surface is oriented we can compute only the contribution of one of the two parallel surfaces (e.g. internal). The MAPT is then created by computing the map at varying $R$, scaling the value of the function by a factor

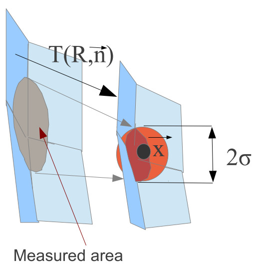


**Figure 1:** *Area projection transform: parallel surface of S at distance R (only in a selected direction or both directions) is estimated. The transform in a point $\vec{x}$ is the area of the original surface generating the part of the parallel one falling inside a sphere of radius σ centered in $\vec{x}$.*



DOI: 10.2312/conf/EG2013/short/013-016

$1/4\pi R$ and using a radius dependent $\sigma$:

$$MAPT(x,y,z,R,S) = \alpha(R)\, APT(x,y,z,S,R,\sigma(R)) \quad (2)$$

where $\alpha(R) = 1/4\pi R^2$ and $\sigma(R) = c \cdot R \quad (0 < c < 1)$. With these choices we obtain a function with maxima non depending on the scale, but only related to the degree of symmetry (see [GL12]). The function can be easily implemented estimating its values for sampled radii on a regular grid.

The joint multiscale map $JMAPT(\vec{x},[r_{min},R_{max}])$ is finally a 3D function computed as the maximal value of the function in the scale range and represents compactly the local degree of symmetry. When computing this map on a regular grid, the scale corresponding to maximal "symmetry" value for each location can be stored as well in a grid of the same size $S_{MAPT}(\vec{x})$.

## 3. Centers of Approximate Spherical Symmetry

Once the MAPT or the JMAPT of a shape is computed, it is possible to extract its salient points, e.g. maxima of the 4D or 3D map. The procedure is rather simple. First local maxima of the function higher than a given threshold are extracted. Maxima that are closer to other ones with similar scale and higher values can be optionally removed from the list. The points obtained represent loci of maximal "approximated" spherical symmetry where the parameter $\sigma(R)$ used in the APT defines the amount of deviation from the perfect sphericity that is tolerated.

A good property of these points that we call "Centers of Approximate Spherical Symmetry" (CASS) is that they are approximately pose independent for articulated shapes and roughly corresponding in similar bodies. Each point is characterized by an intensity value (e.g. the degree of symmetry) and a scale (e.g. the radius of the local symmetry). Furthermore, we add other three descriptor components by estimating the spatial behavior of the map around the points. Actually, if $R_M$ is the scale of the maximum, we computed the inertia matrix of the MAPT at radius $R_M$ and in region of size $R_M$ and compute from its eigenvalues the sphericity, elongation and flatness of the map. Not that we could as well compute these parameters when building the MAPT on a discretized grid, storing in dedicated accumulators also the normal direction (this procedure creates, however a huge memory overhead). The point description obtained, given by a 5-components vector can be sufficient to recognize specific points of a shape (e.g. head or trunk of a human body that have unique scale or peculiar sphericity), but it is not sufficient to allow a reliable point matching between two corresponding shapes. For this reason we tried to better characterize the points and the global shape description building a graph representation. Our idea was to join the salient points following maximal symmetry path, in this way following centers of approximately cylindrical parts independently on the quality and on the topology of the shape borders.

## 4. Radial Symmetry Graphs

We therefore create our "Radial Symmetry Graph" from the CASS points with the following procedure:

- Join each point of the list with all the others by performing fast marching from the points with speed proportional to the squared symmetry scaled JMAPT value mapped in the range $0.001-1$ and extracting minimal paths [DC01]. This results in lines that tends to follow cylindrical part axes when available otherwise follow minimal euclidean paths. We compute twice paths between two points (switching start/end points) taking as the correct path the shortest one.
- (optional) Clean the graph by removing all the paths that are close to another CASS point different from its extrema. We define a spherical region of influence (ROI) with radius proportional to the scale for each point and test intersection of paths with ROIs of all the points different from their extrema. This procedure removes paths that should in principle be superimposed and provides a way to characterize shapes through graph connectivity.

The structure obtained has some interesting properies:

- It follows tubular parts of the shape: as shown in [GL12] the JMAPT is maximal along cylindrical paths, also robustly against noise and holes.
- It tends to connect these cylindrical centerlines to centers of spherical structure or to corners (creating an approximate spherical symmetry as shown in [GL12])
- Relevant information is encoded in paths. We can use, to match points or entire graphs, not only the information related to node features or to connectivity, but also path similarity, as, for example, done in [BL08].

Note that the complete graphs characterize points (and also entire shapes) only through the paths behavior. The cleaned graphs describe the global objects' properties also through heir connectivity.

## 5. Computing path similarity

Comparing paths connecting CASS points we have a powerful way to characterize locally salient points and complete graphs. Following the approach of [BL08] we can, in fact compute path dissimilarity by summing two contributions. The first depends on symmetry scale difference in $N$ evenly spaced points along the paths ($\vec{p}_1(i)$ for the first path and $\vec{p}_2(i)$ for the other one). The second depends on the difference of the paths lengths $l_1$, $l_2$:

$$d(p_1,p_2)=\sum_{i=1}^{N}\frac{(S_{MAPT}(\vec{p}_1(i))-S_{MAPT}(\vec{p}_2(i)))^2}{S_{MAPT}(\vec{p}_1(i))+S_{MAPT}(\vec{p}_2(i))}+\gamma\frac{(l_1-l_2)^2}{l_1+l_2} \quad (3)$$

Actually to compare our paths we could add also also a JMAPT intensity based dissimilarity component:

$$d'(p_1,p_2)=\sum_{i=1}^{N}\frac{(JMAPT(\vec{p}_1(i))-JMAPT(\vec{p}_2(i)))^2}{JMAPT(\vec{p}_1(i))+JMAPT(\vec{p}_2(i))} \quad (4)$$

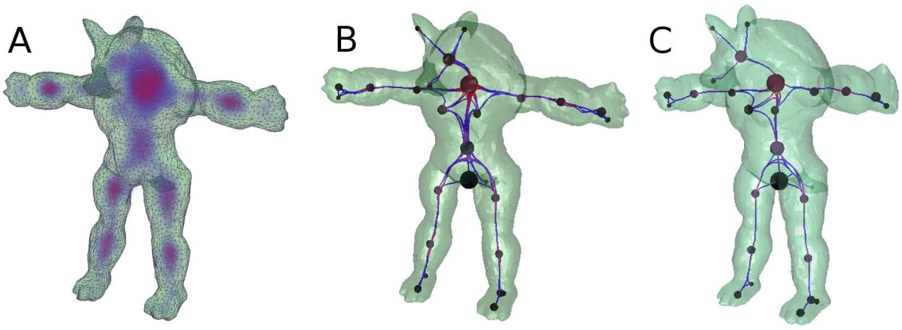


**Figure 2:** *A: Volume rendering of the JMAPT computed on an armadillo mesh. B: CASS points extracted from the map represented as spheres of* $1/4$ *of the corresponding scale, rendered with color coded sphericity and Radial Symmetry Graph joining all the points. C: Same graphs simplified by removing paths too close to salient points different from their extrema.*

Scale information, however, should be more robust against holes with respect to signal intensity, component directly depending on the amount of surface projected in the point. We therefore used only $d(p_1, p_2)$ in our tests. Lengths and scales should be approximately pose independent and characterize well the shape.

## 6. Applications

Once salient points, graphs, paths and path comparison metrics are available, we can use them for differene practical applications, like points matching, semantic labelling of points, graph matching and intrinsic symmetry detection. Let us briefly describe the approaches we are trying to follow for these tasks.

### 6.1. Points matching and semantic labelling

CASS points computed on models differing for an articulated deformation are mostly stable they and are rather similar in objects of the same type (e.g. humans, animals). We can therefore try to match them, and even if the local characterization is poor, we can exploit for the task descriptors based on the similarity of paths starting from each point (e.g. average/median path distances, histograms of paths length or paths features) to characterize them with a robust contextual information. We plan to test several descriptors of this kind as future work. In the meanwhile we implemented a simple "counting" procedure to match corresponding points of two graphs extracted on similar objects. Given a new graph and a template one we perform the following steps:

- initialize a counter for each label at each point
- for each path of the new model search for the nearest neighbor among the paths extracted on the template and increment the counters of the extremal points corresponding to the labels of the corresponding points of the closer path of the template.
- select as the best match the point with the maximally valued counter

A problem of this procedure, and of all the point matching procedure is that they cannot distinguish between symmetric parts creating points with similar paths. We can, however, modify the procedure performing just a semantic labelling of the point set, using in the procedure non unique labels for the template points identifying simply a point type (e.g. leg, back, head, ear, etc).

### 6.2. Graph matching

It is, however, also possible to perform a complete graph matching, even if CASS points are not completely corresponding in the couple of models. Several methods have been in fact presented in literature to perform this task, even for partial matching or in presence of outlier. For example, if we consider the "cleaned" graph where also the connection define a meaningful structure, we can apply classical graph matching methods as usually done in many applications [TKR08,SSGD03] and obtain at least a robust labelling of the highest valued salient points. Also the previously described "counting" technique can be modified in order to enforce spatial relationships between nodes. A solution can be simply to consider not simple best matches between single paths, but matches between couple of paths with compatible distances between corresponding nodes. We plan to test different approaches on a well defined testbed in the near future.

### 6.3. Detection of intrinsic symmetries

Another simple application of paths comparison can be the detection of intrinsic symmetries [MBB10]. In fact intrinsically symmetrical CASS points should be characterized by a similar set of connections. We can detect intrinsic symmetries through the similarity of sets of paths starting from two different CASS points separated by long paths. We plan to test the same point similarity measures used to match points in corresponding models to detect intrinsic symmetries on single models.

## 7. Preliminary results

Figure 3 shows examples of CASS salient points and corresponding "cleaned" symmetry graphs. It is possible to see

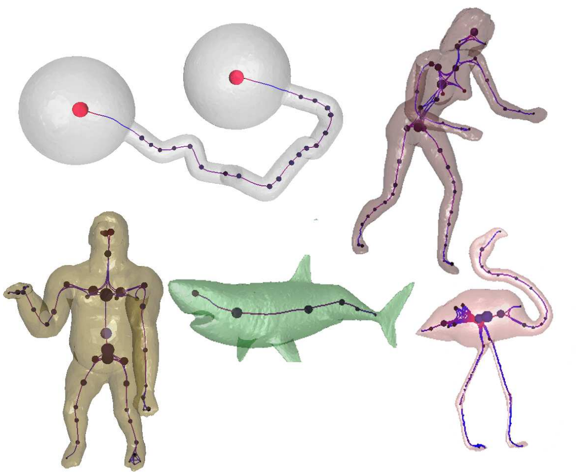

**Figure 3:** *Examples of cleaned Radial Symmetry Graphs computed on different shapes.*

that they resemple curve skeletons in tubular parts, but characterize also the other parts linking salient points and their computation is robust against noise and holes. A limit in the possibility of using points and paths for matching is surely related to the fact that in articulated shapes a few salient points can be created by the pose (see the shark in Fig. 3). Most of CASS are, in any case stable in different poses, as shown in Fig. 4.

We tested the semantic labelling obtained with the simple "voting" procedure on a set of models from the SHREC 2011 nonrigid watertight dataset [LGB*11]. Labelling the salient points of the template model of an armadillo as head, trunk, back, arms, legs, nose, ear, chest, pelvis we were able to assign the right labels to more than 90% of the 15 CASS points of other 10 models deformed through an articulated transform (Fig. 4) using the labels manually given to a single template (pose of Fig. 2) as example.

## 8. Discussion

We proposed a new robust characterization of shapes based on the extraction of salient points (CASS) computed from the Joint Multiscale Area Projection Transform and the creation of a graph (Radial Symmetry Graph) obtained by joining these points following maximal JMAPT paths. This shape characterization inherits the robustness against noise, holes and topological changes of the original transform. The graph structure can be useful for matching purposes adding contextual information to the point characterization and could also be applied to intrinsic symmetry detection. In a first test we were able to assign a semantic label to salient points of articulated objects in different poses from a labelled example, using a simple path distance based voting. We plan to implement and try all the applications here proposed on real world data and on public datasets, to verify if they can provide good results on relevant tasks.

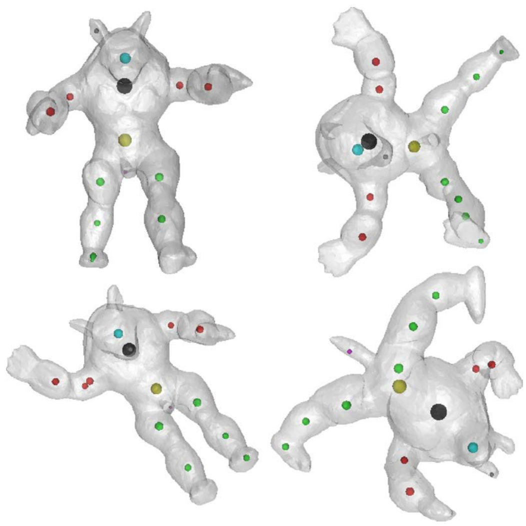

**Figure 4:** *Automatic labelling of the highest valued 15 CASS points for armadillos in different poses obtained from a single manually labelled template.*

## References


[BL08] BAI X., LATECKI L.: Path similarity skeleton graph matching. *Pattern Analysis and Machine Intelligence, IEEE Transactions on 30*, 7 (july 2008), 1282 –1292. 2

[CSM07] CORNEA N. D., SILVER D., MIN P.: Curve-skeleton properties, applications, and algorithms. *IEEE Transactions on Visualization and Computer Graphics 13*, 3 (2007), 530–548. 1

[DC01] DESCHAMPS T., COHEN L.: Fast extraction of minimal paths in 3d images and applications to virtual endoscopy. *Medical Image Analysis 5*, 4 (2001), 281–299. 2

[GL12] GIACHETTI A., LOVATO C.: Radial symmetry detection and shape characterization with the multiscale area projection transform. *Comp.Graph.Forum 31*, 5 (2012), 1669–1678. 1, 2

[LGB*11] LIAN Z., GODIL A., BUSTOS B., ET AL.: Shrec'11 track: shape retrieval on non-rigid 3d watertight meshes. In *Proc. Eurographics/ACM SIGGRAPH Symposium on 3D Object Retrieval* (2011), pp. 79–88. 4

[MBB10] MITRA N. J., BRONSTEIN A., BRONSTEIN M.: Intrinsic regularity detection in 3d geometry. In *Proceedings of the 11th European Conference on Computer Vision: Part III* (Berlin, Heidelberg, 2010), ECCV'10, Springer-Verlag, pp. 398–410. 3

[MGP10] MIKLOS B., GIESEN J., PAULY M.: Discrete scale axis representations for 3d geometry. *ACM Transactions on Graphics (TOG) 29*, 4 (2010), 101. 1

[SF06] SHILANE P., FUNKHOUSER T.: Selecting distinctive 3D shape descriptors for similarity retrieval. In *Shape Modelling and Applications* (2006), IEEE Computer Society, p. 18. 1

[SSGD03] SUNDAR H., SILVER D., GAGVANI N., DICKINSON S.: Skeleton based shape matching and retrieval. In *Proc. Shape Modeling International* (Washington, DC, USA, 2003), IEEE Computer Society, pp. 130–. 3

[TKR08] TORRESANI L., KOLMOGOROV V., ROTHER C.: Feature correspondence via graph matching: Models and global optimization. In *Proceedings ECCV 2008*, Forsyth D., Torr P., Zisserman A., (Eds.), vol. 5303 of *LNCS*. Springer Berlin Heidelberg, 2008, pp. 596–609. 3